Employing the phase in master slave interferometry

Sylvain Rivet[b], Adrian Bradu[a] and Adrian Podoleanu*[a]
[a]Applied Optics Group, School of Physical Sciences, University of Kent, Canterbury CT2 7NH, UK
[b]Université de Bretagne Occidentale, IBSAM, Laboratoire OPTIMAG, 6 avenue Le Gorgeu, C.S. 93837, 29238 Brest Cedex 3, France

ABSTRACT

In this paper, we extend the master slave (MS) method, so far applied to the modulus of the spectra acquired in spectral domain interferometry, to processing complex spectra. We present the algorithm of complex master slave interferometry (CMSI) method and illustrate the importance of phase processing for signal stability and strength. We demonstrate better stability of the signal driving a direct *en-face* OCT image by processing both real part and imaginary part of the CMS signal. Then we show that by processing the phase, novel avenues can be opened for the master slave method. A first avenue detailed here is that of dispersion measurements.

Keywords: master slave, phase measurements, dispersion, group velocity, optical coherence tomography

1. INTRODUCTION

The key value of spectral (Fourier) domain interferometry (SDI) is its ability to encode spatial data into the spectrum at the interferometer output. There are two modalities on transducing this information from the optical domain into electrical: spectrometer-based interferometry where a broadband optical source is employed together with a spectrometer and swept source-based interferometry, where a tunable (swept) laser is used and signal is delivered by a photo-detector. Both methods are characterized by nonlinearities in transferring the modulation of the optical spectrum into an electrical signal. Such nonlinearities lead to an irregular modulation (chirp) of the electrical signal read out by the spectrometer or the photo-detector while tuning the laser respectively. These nonlinearities can have two origins: the readout specificities (nonlinearities in the spectrometer or in the tuning of the swept source) and unbalanced dispersion in the interferometer and sample. Unless this chirp is compensated for, a Fourier Transform (FT), applied to the electrical signal proportional to the channeled spectra, leads to a wider and reduced amplitude of the reflectivity profile peaks.

To avoid the disadvantages mentioned above, stemming from the use of FTs, the master/slave method was proposed by Podoleanu et al. [1], to which we are referring as the Master Slave Interferometry (*MSI*) method. This method is based on comparing raw acquired spectra from the sample with experimentally measured spectra (real-value experimental masks M_{exp}) using a mirror, placed in the interferometer at equivalent OPD values where information from the sample is needed. By not performing a FT, a radical change in data processing is established. Initially, the amplitudes of the spectra were compared only via correlation methods. This meant that the phase was discarded. The initial application of the method was further improved to Complex Master Slave Interferometry (*CMSI*) [2] where the processing of complex signals allows phase recovery. *CMSI* was extended to improve the calibration stage of the method, wherefrom a reduced number of experimentally acquired channeled spectra using a mirror, any number of masks are theoretically inferred (complex-value inferred masks M_{built}). *CMSI* allows novel avenues by providing more than a mask per resolution interval and calculation of any number of masks becomes possible. So far only the advantage of calculating the masks was reported in producing an OCT/SLO instrument for the eye [3], coherence revival [4], BCC of eye lids [5], Gabor filtering [6], embryology [7]. The given access to phase processing.

We demonstrate better stability of the A-scan signal, that in fact in the context of the *CMSI* signifies better stability of the signal that leads to a direct *en-face* OCT image. This was only illustrated in the initial report [2], but not used. The better stability is the consequence of processing both real part and imaginary part of the *CMSI* signal. Then we show that by processing the phase, novel avenues can be opened for the master slave method. A first avenue detailed here is that of dispersion measurements, as published in [8].

In the continuation of the manuscript, we will show how phase can be recovered using the *CMSI*, demonstrate the stability of the recovered phase with respect to the conventional *MSI* approach, and then demonstrate a technique to measure dispersion properties of various samples by using an "ideal" interferometer. This interferometer is perfectly compensated for unbalanced dispersion and corrected for non-linearities via the *CMSI* technique. By using such an ideal

interferometer, any phase alteration due to insertion of an investigated sample is exclusively related to the sample dispersion.

2. PHASE RECOVERY IN CMSI IMPLEMENTATION

Let us consider the pixel position (x) on the spectrometer camera and the optical path difference (OPD = δ) in the interferometer. *CMSI* consists in calculating a discrete integral between the electrical signal I(x,δ), converting the channeled spectrum at the output of the interferometer, and the complex-value inferred masks, M_{built}, as follows:

$$CMSI\left[I\left(x,\delta\right)\right]=\sum_{i=1}^{N}I\left(x_i,\delta\right)M_{built}^{*}\left(x_i,t\right)=FT^{-1}\left[I^{\,without\ chirp}\left(\omega,\delta\right)\right] \tag{1}$$

where ω is the optical angular frequency and the symbol * signifies complex conjugate. The result is equivalent to an inverse Fourier transformation (FT^{-1}) of the complex signal created by reading the channeled spectra $I^{without\_chirp}$ expressed according to:

$$I^{\,without\ chirp}\left(\omega,\delta\right)=I_0\left(\omega\right)Exp\left[i\phi\left(\omega,\delta\right)\right] \tag{2}$$

The ultimate quantity to be obtained is the phase of the signal $I(x,\delta)$, $\phi(\omega,\delta)$. Using *CMSI* there is no need to resample the channeled spectra nor remove the uncompensated chirp because the channeled spectra are expressed as a combination of local oscillators (masks) according to δ, spectra that already contain the chirp measured at the Master stage. The masks represent eigenfunctions of the OCT operator that returns as eigenvalues, the reflectivity values within the A-scan at different depths. Thus, by calculating the Fourier transform and the argument of *CMSI*[*I*] (Fig. 1), it is possible to extract the phase $\phi(\omega,\delta)$ as:

$$\phi\left(\omega,\delta\right)=Arg\left[I^{\,without\ chirp}\left(\omega,\delta\right)\right]=Arg\left[FT\left[CMSI\left[I\left(x,\delta\right)\right]\right]\right] \tag{3}$$

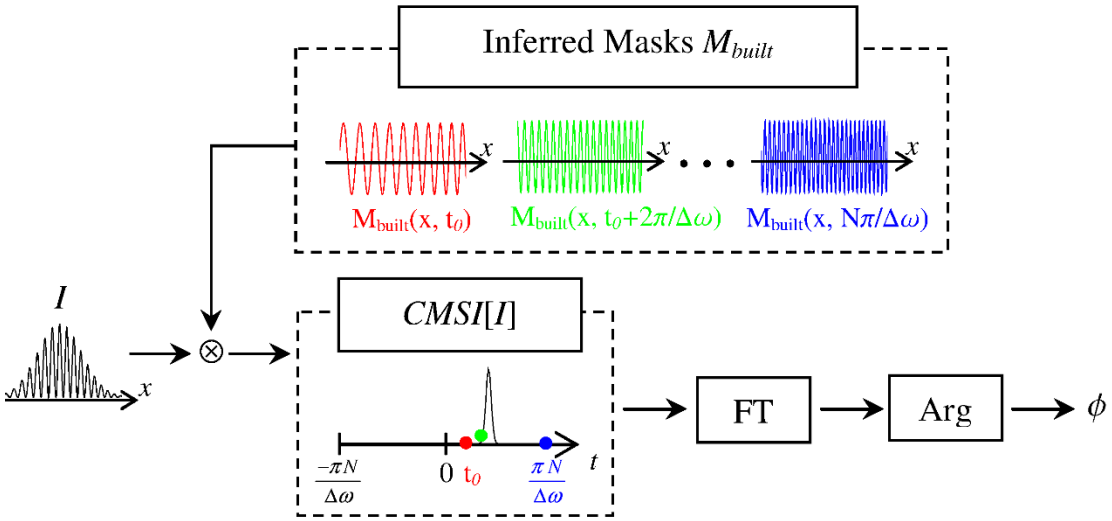

Fig. 1. Block diagram showing the procedure of extracting the spectral phases ϕ from the channeled spectra *I*. Inferred masks M_{built} and *CMSI*[*I*] are complex quantities, only their amplitudes are represented in this diagram.

3. STABILITY STUDY AND SIGNAL DROP-OFF IN DEPTH: COMPARISON BETWEEN MSI AND CMSI

In order to illustrate the insensitivity of *CMSI* to the random phase shifts, several A-scans have been recorded over time while imaging a flat mirror. The interferometer used in this experiment is that of an OCT interferometer driven by a swept source, where the digitizer is not synchronized by the source k-clock, but by its internal clock generator.

The sampling in depth is chosen equal to 0.4 μm, much denser than the sampling obtained with the FT based method, estimated at 6.1 μm by measuring the displacement of the peak in Fourier domain according to the displacement of the reference mirror. This massive oversampling is implemented in order to determine a well-defined reflectance profile, to accurately measure the peak width (9.0±0.2 μm here).

In Fig. 2(a), *MSI* signal has been calculated by using the *MSI* approach based on cross-correlation. The cross-correlation was performed between masks and channeled spectra collected every 2 seconds. To perform the calculation, 100 channeled spectra (CS_{exp}) have been recorded using a mirror as sample from OPD = 500 μm to 540 μm. These 100 CS_{exp} are used as experimental masks. As shown in Fig. 2(a) and in Fig. 2(c) corresponding to reflectance profile for a particular time, the reflectance profile is noisy due to interferometer random phase shifts in the channeled spectra CS_{exp} .

In Fig. 2(b), the absolute value of *CMSI* signal has been calculated from the same raw data previously used for the *MSI*. To perform the calculation, the 100 inferred masks M_{built} distanced at 0.4 μm has been calculated using 2 CS_{exp} measured at OPD = 500 μm and 540 μm. As shown in Fig. 2(b) and by the blue profile in Fig. 2(c) the *CMSI* reflectance profile does not present significant fluctuations.

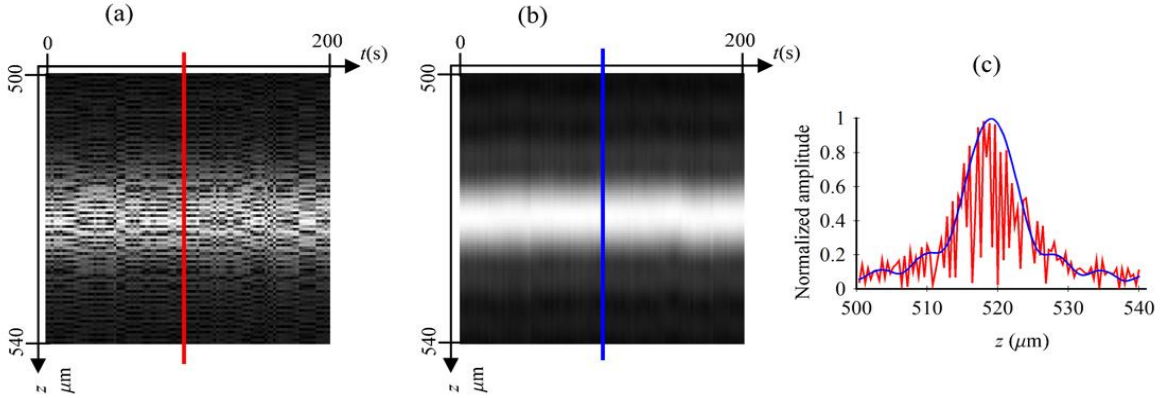

Fig. 2. (a) A-scans (vertical axis) for a mirror as object, represented in time (horizontal axis) calculated with *MSI* and 100 CS_{exp} utilized as masks. (b) A-scans (vertical axis) for a mirror as object represented in time (horizontal axis) calculated with *CMSI* using 100 inferred masks obtained from 2 CS_{exp}. (c) Reflectance profiles calculated by *MSI* (red) and *CMSI* (blue) in a time t = 100 seconds.

4. GROUP INDEX AND DISPERSION MEASUREMENT PROCEDURE

An application of phase processing enabled by *CMSI* is to evaluate material dispersion. This opens two directions of applications, in metrology as well as that of compensating for dispersion variation with depth in OCT samples. We will refer to the first direction in this study.

To validate the accurate recovery of the phase through *CMSI* procedure, group index and dispersion measurement have been carried out. Let us consider two channeled spectra $I^{sample}(x,\delta_s)$ and $I^{vacuum}(x,\delta_v)$ recorded respectively with the sample to be investigated placed in the sample arm of the interferometer, and without. The OPD in the interferometer is adjustable by moving the sample mirror M_s using a translation stage. The corresponding OPDs δ_s and δ_v can be expressed as $\delta_s=2(z_s-z_{s0})$, where z_s is the current position of the sample mirror M_s and z_{s0} is the linear stage position for OPD = 0 with the sample, and $\delta_v=2(z_v-z_{v0})$, where z_v is the current position of the mirror M_s and z_{v0} is the linear stage position for OPD = 0 without the sample respectively. A set of inferred masks M_{built} is built from $M_{built}(x,t_0)$ presenting several cycles over N pixels to the densest mask $M_{built}(x,t_N)$ whose number of the cycles is close to $N/2$ (related to Nyquist frequency). The values t are related to the OPD values where *CMSI* calculation returns a reflectivity point of the reflectivity profile in depth, A-scan.

Let us consider a uniformly-spaced range of t values, with an interval equal to the spatial axial resolution limit, $2\pi/\Delta\omega$ where $\Delta\omega$ is the spectral range of the spectrometer equal to the difference $\Delta\omega = p(x_N) - p(x_1)$, where $p(x) = \omega$. For a line camera of N pixels, according to Nyquist, only $N/2$ cycles in the channeled spectrum can be sampled. This determines a range of $\pi N/\Delta\omega$ of t values along the OPD coordinate, to accurately represent the A-scan. $CMSI[I^{vacuum}]$ and $CMSI[I^{sample}]$ are defined with N values in time domain with an interval equal to $2\pi/\Delta\omega$. All values are equal to 0 except those

corresponding to the product between the I^{vacuum} (and I^{sample}) with the set of masks M. The first mask does not start with a zero-cycle over the N pixels to remove the DC component of the channeled spectra

The instantaneous phases ϕ^{sample} and ϕ^{vacuum} related to I^{sample} and I^{vacuum} can be measured according to the procedure described in Fig. 1 and the phase difference $\Delta\phi=\phi^{sample}-\phi^{vacuum}$ is calculated. The dependence $\Delta\phi$ vs ω can be fitted by a quadratic form:

$$\Delta\phi(\omega)=\alpha+\beta(\omega-\omega_c)+\gamma(\omega-\omega_c)^2 \tag{4}$$

where ω_c is the angular frequency at the center of the spectrum and where coefficients β and γ are connected to the group index n_g and group velocity dispersion GVD as follows:

$$n_g(\omega_c)=\frac{c\beta/2+z_v-z_s}{e}+1, \tag{5}$$

$$GVD(\omega_c)=\frac{\gamma}{e}, \tag{6}$$

with e the thickness of the sample.

5. RESULTS & DISCUSSION

A flint glass sample SF6 is used of 20 mm thickness whose catalogue data gives a group index n_g=1.8205 and group velocity dispersion GVD=173.37 fs^2/mm at the central pixel of the camera ω_c=2.145 rad.fs^{-1}, *i.e.* λ_c = 0.8788 μm.

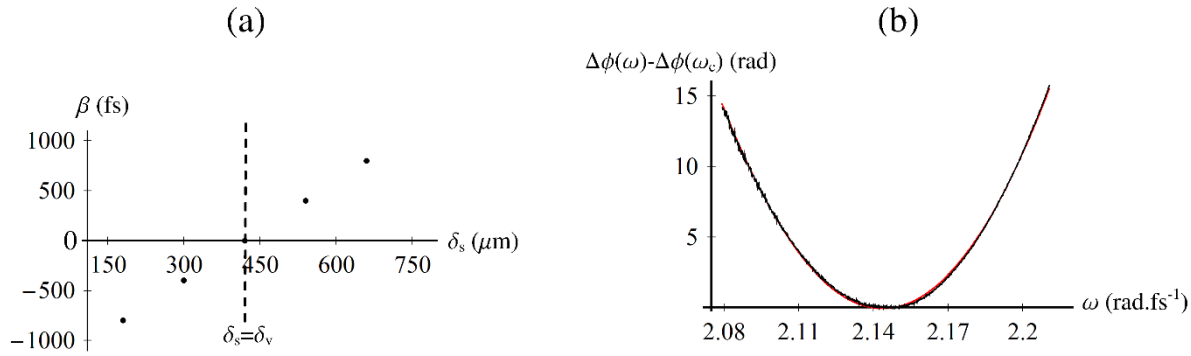

Fig. 3. Measurement with a 20 mm- thick SF6 glass. (a) Coefficient β corresponding to the linear term of the phase difference Δφ versus OPD δ_s (by changing the length of the sample arm). (b) Δφ-Δφ(ω_c) is displayed in black curve between 2.08 and 2.2 rad.fs^{-1} for the particular case β≈0 with z_v = 20.1 mm and z_s=3.695 mm. The red curve corresponds to the fit of Δφ-Δφ(ω_c) with β=(13±8)fs and γ=(3470±30)fs^2, which leads to n_g=1.8203 +/- 0.0001 and GVD=(173 +/- 2) fs^2/mm.

The channeled spectrum I^{vacuum} is recorded without the glass being placed in the sample arm of the interferometer for the position of the mirror M_s moved along the optical axis by a linear stage, z_v = 20.1 mm. When the glass is placed in the sample arm, the mirror M_s is adjusted so that the main spectral modulation of the channeled spectrum I^{sample} is similar to that of I^{vacuum} (z_s=3.695 mm), *i.e.* the OPDs δ_s and δ_v are identical, which means coefficient β≈0 (Fig. 3(a)). I^{vacuum} and I^{sample} are recorded 10 times in order to assess the accuracy of n_g and GVD measurements given in the form of (mean +/- 2 standard deviation). Because fringe visibility is very weak at the edge of the spectra, Δφ - Δφ(ω_c) is not plotted over the all spectrum range. A fit by a quadratic polynomial centered at ω_c, leads to n_g=1.8203 +/- 0.0001 and GVD=(173 +/- 2) fs^2/mm (Fig. 3(b)). The experimental results are in good agreement with the theoretical values. The consistent deviation between the experimental and theoretical values of n_g can be explained by the accuracy in measuring the thickness of the sample. If a 19.995 mm-sample was considered, then a perfect match with the theoretical value of n_g would be obtained.

To assess the stability of the measurements, *GVD* and n_g have been evaluated for different positions of the mirrors M_s and M_r, such as the OPDs with the sample (δ_s) and without the sample (δ_v) are always identical. In this case the variations of *GVD* and n_g are inferior to the standard deviation, which proves the robustness of the *CMSI* method.

6. CONCLUSIONS

This paper demonstrates that the CMSI method used in SDI can efficiently be used for accurate refractive index and group velocity dispersion measurements of optically transparent samples. The method uses a continuous range of frequencies, while other methods have been reported using measurements at discrete optical frequency values [9].

Based on the results presented in this paper, other avenues are foreseeable, such as extending the CMSI method towards a matrix approach (please see the paper [10]), as well as utilization of phase recovered via the CMSI method for phase sensitive OCT and for polarization sensitive OCT. Future work should refer on how phase accuracy evolves with OPD, in the context of longer axial range proven by the CMSI [11] in comparison with conventional signal processing methods. A recent report [12] has proven the consistency of high-resolution distance measurements when using CMSI. We expect that this conclusion can be extended to phase measurements, but a demonstration remains to be reported.

ACKNOWLEDGMENTS

The authors wish to acknowledge the following funding sources: H2020 Marie Sklodowska-Curie Actions (MSCA) (625509), Engineering and Physical Sciences Research Council (EPSRC) (`REBOT', EP/N019229/1), H2020 European Research Council (ERC) (`ADASMART', 754695), National Institute for Health Research Biomedical Research Centre at Moorfield Eye Hospital NHS Foundation Trust (NIHR), the UCL Institute of Ophthalmology, University College London, and the Royal Society Wolfson research merit award.

REFERENCES

[1] Podoleanu A., and Bradu, A., "Master-slave interferometry for parallel spectral domain interferometry sensing and versatile 3D optical coherence tomography," Opt. Express 21(16), 19324–19338 (2013).
[2] Rivet, S., Maria, M., Bradu, A., Feuchter, T., Leick, L., Podoleanu, A., "Complex Master Slave Interferometry," Opt. Express 24(3), 2885-2904 (2016).
[3] Bradu, A., Kapinchev, K., Barnes, F., Podoleanu, A., "Master slave en-face OCT/SLO," Biomed. Opt. Express 6, 3655-3669 (2015).
[4] Bradu, A., Rivet, S., and Podoleanu, A., "Master/slave interferometry – ideal tool for coherence revival swept source optical coherence tomography", Biomed. Opt. Express 7, 2453-2468 (2016).
[5] Chin, C. et al., "Master/slave optical coherence tomography imaging of eyelid basal cell carcinoma", Appl. Opt. 55, 7378-7386 (2016).
[6] Cernat, C. et. al., Gabor fusion master slave optical coherence tomography, Biomed. Opt. Express 8, 813-827 (2017).
[7] Caujolle, S., Cernat, R., Silvestri, G., Marques, M., Bradu, A., Feuchter, T., Robinson, G., Griffin, D., and Podoleanu, A., "Speckle variance OCT for depth resolved assessment of the viability of bovine embryos Biomed". Opt. Express 8, 5139-5150 (2017).
[8] Rivet, S., Bradu, A., Bairstow, F., Forrière, H., and Podoleanu, A., "Group refractive index and group velocity dispersion measurement by complex master slave interferometry", Opt. Express 26, 21831-21842 (2018).
[9] Kolenderska, S.M., Bräuer, B.,and Vanholsbeeck, F., "Dispersion mapping as a simple postprocessing step for Fourier domain Optical Coherence Tomography data", *Scientific Reports,* **8**-9244 (2018).
[10] Podoleanu, A., Bradu, A., Marques, M., and Rivet, S., "Speeding up master slave optical coherence tomography by matrix manipulation", Big Data, Photonics West Conference, (2019).
[11] Marques, M., Rivet, S., Bradu, A., and Podoleanu, A., "Complex master-slave for long axial range swept-source optical coherence tomography," OSA Continuum 1, 1251-1259 (2018).
[12] Bradu, A., Israelsen, N., Maria, M., Marques, M., Rivet, S., Feuchter, T., Bang, O., and Podoleanu A., "Recovering distance information in spectral domain interferometry", Sci Rep 8, 15445 (2018).